J Mol Model (2011) 17:3057–3062
DOI 10.1007/s00894-011-0980-0

ORIGINAL PAPER

High pressure phase transition and elastic properties of covalent heavy rare-earth Antimonides

Purvee Bhardwaj · Sadhna Singh

Received: 4 October 2010 / Accepted: 21 January 2011 / Published online: 1 March 2011

Abstract In the present paper, we report an investigation into the high-pressure structural phase transition of rare earth antimonides (DySb and ErSb). A modified interaction potential model (MIPM) (including the covalency effect) has been developed. Phase transition pressures are associated with a sudden collapse in volume, indicating the occurrence of a first order phase transition. At compressed volumes, these compounds are found in the CsCl phase. The phase transition pressures and associated volume collapses obtained from the potential model developed here show a generally better agreement with available experimental data than others available in the literature. The elastic constants and bulk modulus are also reported. Our results are, in general, in good agreement with experimental and theoretical data where available, and provide predictions where data are unavailable.

PACS 62.20.de · 62.20.dq · 62.50.-p · 64.00.00

Keywords Semiconductor · Phase transition · Thermodynamic property · Mechanical property

Introduction

Rare-earth monopnictides are generally semiconductors or semimetals. Despite their simple rock salt structure, they demonstrate various types of magnetic ordering, generally with low transition temperatures. Their electronic structures and magnetic properties are sensitive to temperature, pressure and impurity effects. The rare-earth 4f–5d interactions and the hybridizations between the rare-earth non-4f and pnictogen p states are responsible for many fascinating phenomena that occur in rare-earth monopnictides. Due to the unfilled 4f shells of rare-earth atoms, it is a challenging problem to obtain an accurate theoretical description of the electronic structure of rare-earth compounds [1–4]. Despite the fact that the 4f energy levels often overlap with the non-4f broad bands of the system, they generally form very narrow resonances, and are often treated as core states in theoretical studies. Due to the highly localized nature of the 4f electrons, the direct f–f interactions between neighboring rare-earth atoms are generally considered to be nearly negligible. Among nitride, phosphide, arsenide, antimonide and bismuthide there is a gradual increase in metalicity in the rare-earth monopnictides. The typical carrier concentrations make them semimetals or highly doped n-type semiconductors [5].

The structural analysis of rare-earth monopnictides under high pressure is an important area of study. The X-ray diffraction profile shows the NaCl-type structure at ambient pressure, whereas under pressure they show a B1–B2 type transition. In these transitions, the compression of the heavy rare-earth atoms bring the 4*f* electrons into play so that these atoms behave more like the lighter rare-earth elements. The rare-earth element is less compressible than the other element of these compounds. So pressure reduces the size of this element more than it reduces the size of the rare-earth. Relative sizes are thus restored to those prevailing for the lighter rare-earths at atmospheric pressure.

Among the rare-earth pnictides, the rare-earth antimonides (LnSb) have recently attracted particular interest as a proper reference material for understanding of various elastic, structural and magnetic effects [6–8]. Some of them

P. Bhardwaj (✉) · S. Singh
High Pressure Physics Laboratory, Department of Physics,
Barkatullah University,
Bhopal 462026, India
e-mail: purveebhardwaj@gmail.com

S. Singh
e-mail: drsadhna100@gmail.com

show magnetic and crystallographic phase transitions at low temperatures. Monoantimonides (CeSb, SmSb and YbSb) with NaCl-type structure, exhibit anomalies in various physical properties due to the p–f mixing, dense Kondo effect and heavy fermion state. Their carrier concentrations increase with decreasing temperature since the p–f mixing becomes stronger. On the other hand, other rare-earth monoantimonides behave as a nearly normal magnetic semi-metals, and display almost temperature-independent carrier concentrations [6–9]. The magnetic properties of NdSb, GdSb, TbSb, DySb, HbSb and ErSb have been investigated by Missell et al. [10] under hydrostatic pressure. They concluded that the magnetic properties of DySb are strongly P-dependent, whereas those of HoSb are P-independent, but sample-dependent. Sapiro et al. [11] studied the crystal field parameters and phase transitions in ErSb.

Pagare et al. [12] investigated the high pressure structural phase transition and cohesive properties of DySb heavy rare-earth mono antimonide by using two-body interionic potential with necessary modifications to include the effect of using two-body coulomb screening by the delocalized 4f-electrons of the rare-earth ion. The structural, elastic and thermal properties of ErSb have been investigated theoretically by using an interionic potential theory consisting of long range coulomb, short range repulsive and van der Waals interaction by Soni et al. [13]. Both these investigations are based on the two-body effect, ignore the charge transfer mechanism, and failed to explain the Cauchy discrepancy. In the series of theoretical investigations, no first principle calculations were done to study the phase transition and elastic properties of DySb and ErSb. Thus, there is a need to study the structural and elastic properties of these compounds.

In addition to the use of synchrotron radiation, the powder X-ray diffraction of LnSb has been studied systematically up to 40 GPa at room temperature by Shirotani et al. [14, 15]. The structure of high pressure phases of LnSb is classified into three groups. The lighter LnSb (Ln=La, Ce, Pr, and Nd) have a tetragonal structure (distorted CsCl type) at high pressures. The high pressure form of the middle LnSb (Ln=Sm, Gd, and Tb) is unknown. The heavier LnSb (Ln=Dy, Ho, Er, Tm and Lu) show the typical NaCl-CsCl (B1-B2) transition at high pressures, though the same transition is not observed in the heavier LnP and LnAs. The transition pressures of LnSb increase with decreasing lattice constant in the NaCl type structure and do not depend on the structure of their high pressure phases.

As we have already stated that the metallization in rare-earth monopnictide increases from nitride to bismuthide, there is a need to include covalency effects for the study of these compounds. Looking at the interesting properties of these less explored rare-earth antimonides, and considering that no work has been done with the potential model including covalency effects, we thought it pertinent to apply a modified interaction potential model (MIPM) that includes the covalence effect in the potential model. The importance of the covalence effect in rare-earth monoantimonides has already been emphasized by Pagare et al. [12] and Vaitheeswaran et al. [3]. Vaitheeswaran et al. reported that their results on bulk moduli under high pressure is doubled, which may be due to an increase in the number of covalent bonds. Pagare et al. [12] found a discrepancy in their results on pressure derivatives of bulk moduli and reported the main reasons for this being the partial covalent nature of these rare-earth monoantimonides. Shirotoni et al. [16] has also confirmed the covalent character of chemical bonds between Dy and Sb atoms.

The present MIPM consists of Coulomb interactions, three-body interactions, van der Waals interaction, overlap repulsive interactions and covalent interactions. The need of inclusion of three-body interaction forces has been stressed by many workers to give better matching of results [17–19]. It was concluded that possible reasons for disagreements include the failure of the two-body potential model, since these studies were based on two-body potentials and could not explain Cauchy violations ($C_{12} \neq C_{44}$). They remarked that results could be improved by including the effect of the non-rigidity of ions in the model.

The aim of this work was to add some additional information to the existing data on the physical properties of two antimonides (DySb and ErSb) theoretically. The main purpose of this work is to investigate the structural and elastic properties of DySb and ErSb. The rest of this

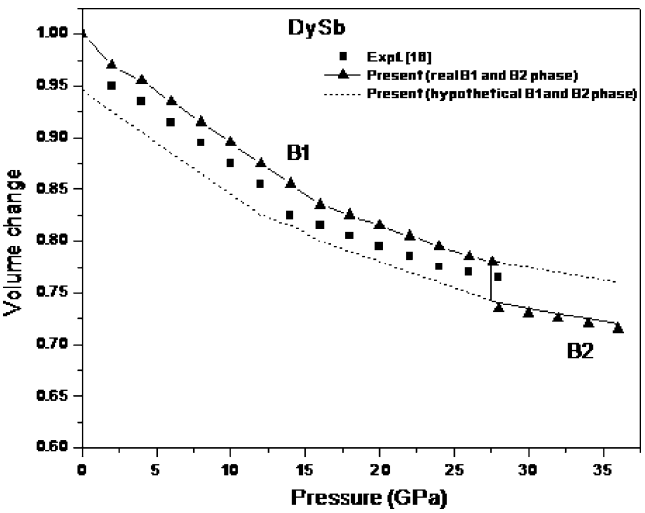

Fig. 1 Variation of volume change V_P/V_0 with pressure for DySb (*solid lines + triangles*). *Solid lines + symbols* real B1 and B2 phases, *dashed lines* hypothetical B1 and B2 phases, *squares* experimental data

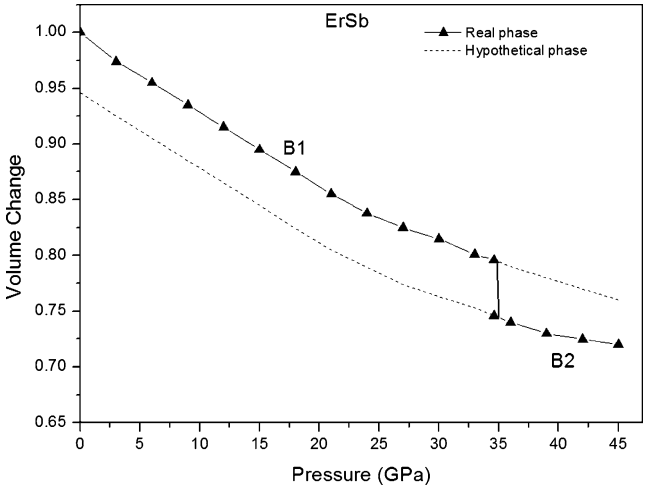

Fig. 2 Variation of volume change V_P/V_0 with pressure for ErSb

paper is organized as follows: the method of calculation is given in the section on Potential model and method of calculation; the results and conclusion are then presented and discussed.

Potential model and method of calculation

The natural consequence of application of pressure on crystals is compression, which in turn leads to an increased charge transfer (or three-body interaction effect) [20] due to the existence of the deformed (or exchanged) charge between the overlapping electron shells of the adjacent ions.

These effects have been incorporated into the Gibbs free energy (G = U+PV−TS) as a function of pressure and three-body interactions (TBI), which are the most dominant among the many body interactions. Here, U is the internal energy of the system equivalent to the lattice energy at temperature near zero and S is the entropy. At temperature T=0K and pressure (P) the

$$G_{BX}(r) = \frac{-\alpha_M{}^X Z^2 e^2}{r^X} - \frac{12\alpha_M{}^X Z e^2 f_m(r)}{r^X} - \left[\frac{C^X}{r^{X6}} + \frac{D^X}{r^{X8}}\right] + 6b\beta_{ij}\exp\left[\left(r_i + r_j - r^X\right)/\rho\right] + 6b\beta_{ii}\exp\left[\left(2r_i - Y_X r^X\right)/\rho\right] + 6b\beta_{jj}\exp\left[\left(2r_j - Y_X r^X\right)/\rho\right] + PV_{BX}(r^X) \quad (1)$$

where X=1 (Phase 1 = B1), 2(Phase 2 = B2), and Y_x= 1.414, 1.154, for NaCl and CsCl structures, respectively.

With $\alpha_m{}^X$ as the Madelung constant, C and D are the overall van der Waal's coefficients for NaCl and CsCl structure, respectively, β_{ij} (i,j=1,2) are the Pauling coefficients defined as $\beta_{ij}=1+(Z_i/n_i)+(Z_j/n_j)$ with Z_i (Z_j), and n_i (n_j) as the valence and the number of electrons of the i(j)th ion. Ze is the ionic charge and b (ρ) are the hardness (range) parameters, r is the nearest neighbor separations $f_m(r)$ is the modified three-body force parameter, which includes the covalency effect with TBI; r_i (r_j) are the ionic radii of ions i (j).

These lattice energies consist of long range Coulomb energy (first term), TBIs corresponding to the nearest neighbor separation r (second term), vdW (van der Waal's) interactions (third term), energy due to the overlap repulsion represented by Hafemeister and Flygare (HF) type potential and extended up to the second neighbor ions (fourth, fifth and sixth terms).

Covalency effects have been included in the TBI in the second terms of lattice energies given by the Eq. 1 parameter according to Motida [21]. Now, the modified three-body parameter $f_m(r)$ becomes

$$f_m(r) = f_{TBI}(r) + f_{\mathrm{cov}}(r) \quad (2)$$

The relevant expressions of f_{TB}, (*r*) and *fcov*(*r*) are given in our earlier work [22, 23].

Structural properties

The B1 (NaCl) structure is the most stable structure in the present compounds, and at high pressure they transform to body-centered B2 (CsCl) structure. As the stable phase is associated with minimum free energy of the crystal, we followed the technique of minimization of Gibb's free energies of real and hypothetical phases. The phase transition occurs when Gibb's free energy difference ΔG approaches zero (ΔG→0). At phase transition pressure (P_t) these compounds undergo a (B1–B2) transition associated with a sudden collapse in volume, indicating a first order phase transition.

We also computed the relative volume changes V(P)/V (0) corresponding to the values of *r* and *r'* at different pressures, and plotted them against the pressure in Figs. 1 and 2 for DySb and ErSb. It is clear from Table 1 and Figs. 1 and 2 that our calculated volume collapse $-\Delta V_{(p)}/V_{(0)}$ for DySb is 6.02% which is close to the result reported by Shirotonin et al. [16] and better than that of Pagare et al. [12]. The negative sign shows the compression in the crystal. The volume collapse $-\Delta V_{(p)}/V_{(0)}$ for ErSb is

Table 1 Phase transition and volume change of DySb and ErSb

Solid	Phase transition pressure (GPa)			Volume collapse %		
	This study	Experimental	Others	This study	Experimental	Others
DySb	27.5	28[a]	23.6[b]	6.02	3.0[a]	6.8[b]
ErSb	34.6	35[a]	33.2[c]	5.60	-	4.7[c]

[a] Ref [16]
[b] Ref [12]
[c] Ref [11]

Table 2 Input data and generated model parameters for DySb and ErSb

Solid	Input parameters			Model parameters		
	r_i(Å)	r_j(Å)	r_0 (Å)	b(10^{-12} ergs)	ρ(Å)	f_m (r)
DySb	0.91[a]	1.25[a]	3.54[b]	14.5083	0.326	-0.01823
ErSb	0.89[a]	1.25[a]	3.50[b]	15.4774	0.315	-0.00454

[a] Ref [27]
[b] Ref [16]

5.6%, which could not be compared with other theoretical or experimental data as they are unavailable.

Elastic and thermophysical properties

We applied the lattice theoretical study of second order elastic constants of cubic crystals by the method of homogeneous finite deformation. The potential is independent of temperature and entropy, so the mechanical elastic constants depend only on the configuration of the crystal. The only condition is that the known potential must be in an analytical form, i.e., it must be a function of the relative positions of the ions in the crystal. The knowledge of second order elastic constants (SOECs) and their pressure derivatives are important for the understanding of the interatomic force in solids. To test the mechanical stability of our model, we computed the elastic properties of the proposed materials. Also, we could reproduce the correct sign of the elastic constants (C_{11}–C_{12}) and C_{44}.

We also calculated the thermo physical properties of the present compounds. The thermo physical properties yield interesting information about substances. Thus, we computed them for DySb and ErSb. The expressions of second order elastic constants used in present work are given in our earlier works [22–24].

Results and discussion

The Gibb's free energies contain three model parameters [b, ρ, $f_m(r)$]. The values of these parameters have been evaluated using lattice parameter, the first space derivatives of the lattice energy (U) and equilibrium condition [25, 26] expressed as:

$$\left[\frac{dU}{dr}\right]_{r=r_0} = 0 \tag{3}$$

$$B_1 + B_2 = -1.165 {Z_m}^2 \tag{4}$$

where, ${Z_m}^2 = Z(Z + 12f(r))$and following methods adopted earlier [22–24]. Using these model parameters and the minimization technique, the phase transition pressures of rare-earth antimonides have been computed. The input data [27] of the crystal and calculated model parameters are listed in Table 2. Figure 3 shows our present computed phase transition pressure for the B1–B2 structure transition in DySb at 27.6 GPa, and ErSb at 34.6 GPa, respectively. The present phase transition pressures are indicated by arrows in Fig. 3 and are listed in Table 1 with their experimental (28 and 35 GPa) and other theoretical (23.6 GPa available only for DySb) results. It is interesting to note that the phase transitions pressures (P_t) obtained from the MIPM model are in general in closer agreement with experimental data [16] and better than the available theoretical results reported by Pagare et al. [12].

At elevated pressures, the materials undergo a structural phase transition associated with a sudden change in the arrangement of the atoms. The atoms are rearranged in new positions, leading to a new structure. Experimentally one usually studies the relative volume changes associated with these compressions. The discontinuity in volume at the transition pressure is obtained from the phase diagram. The compression curves are plotted in Figs. 1 and 2 for DySb and ErSb, respectively. The values of the volume collapses (%) are given in Table 1. Our results on volume collapse are close to available experimental and other results. It is clear that, during the phase transition from NaCl to CsCl, the volume discontinuity in the pressure volume phase diagram identifies the same trend as the other experimental approach. In Figs. 1 and 3, solid lines + symbols represent the real B1 and B2 phases, dashed lines represent the hypothetical B1 and B2 phases. The solid squares represent

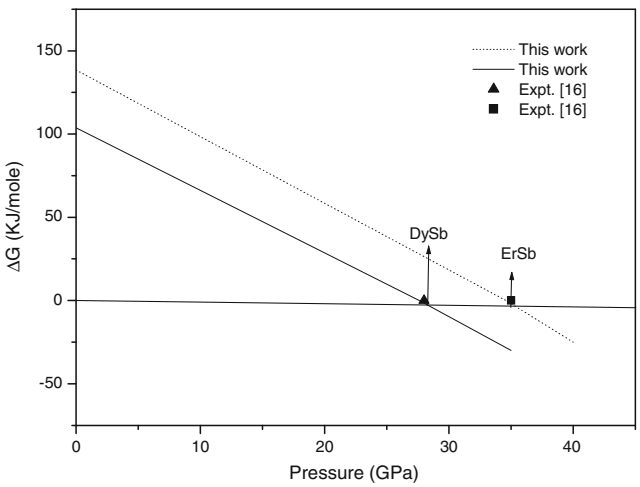

Fig. 3 Variation of Gibb's free energy with pressure for DySb and ErSb

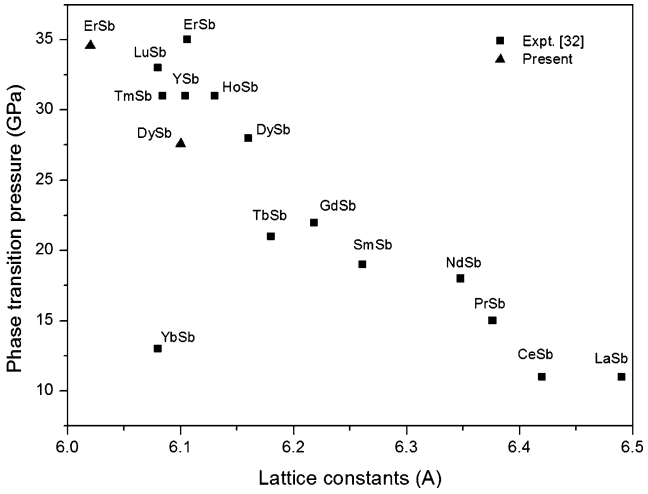

Fig. 4 Variation of lattice constant (*A*) with phase transition pressure for various rare earth antimonides

the experimental data. Figures 1 and 2 show that our potential model can effectively explain the high pressure behavior of these compounds.

To show the relationship between phase transition pressures and lattice constants of antimonides, we display the results for various rare-earth antimonides for lattice constants with phase transition pressure in Fig. 4. It is clear that the phase transition pressures of all the rare-earth antimonides increase with decreasing lattice constant. This decrease occurs with increasing atomic number. The lattice constants of rare-earth monopnictides, as a general trend, increase from N to Bi but decrease from La to Lu: the lattice constant typically decreases with increasing 4f occupancy. This trend in the lattice constant can be simply explained by the increase in anion sizes and the decrease in cation sizes with the increase in atomic number [1, 26]. We have compared our (solid triangles) results with experimental data (solid squares) [16]. Our values generally show the same trend as experimental results [16].

The study of elastic behavior under pressure is well known to supply useful information about changes in the character of the covalent and ionic forces induced in crystal as it is subjected to phase transformation. We calculated the second order elastic constants of the materials under study. Also, we could reproduce the correct sign of the elastic constants (C_{11}–C_{12}). The study of SOECs under pressure is important as C_{11} represents elasticity in length, and C_{12} and C_{44} are shape-related elastic constants. The SOECs of rare-earth antimonides have been calculated and are listed in Table 3. Our present values of SOECs are close to available theoretical data [2, 12, 13], and the values of SOECs given by Mullen et al. [2] at 200 K. Due to lack of experimental data for SOECs, we compared our results with theoretical data but the values of SOECs are of the same order as reported by others [2, 12, 13]. To the best of our knowledge, no experimental data of second order elastic constants for these rare-earth antimonides have yet been reported.

Moreover, our present model is able to explain the Cauchy violation. One common approach is to assume that the atoms are connected with springs and that the resulting forces are only in the direction of the nearest neighbors (central force model). The deviation from the Cauchy violation $\delta = c_{12} - c_{44} - 2P$ is a measure of the contribution from the non-central many-body force. The calculated values of Cauchy violation are given in Table 3 for DySb and ErSb. The sign of δ justifies the values of C_{12} and C_{44}.

In order to understand the thermo physical properties, we calculated the Debye temperature. The Debye characteristic temperature, θ_D, reflects its structure stability, the strength of bonds between its separate elements, structure defects availability and its density. The calculated values of Debye temperatures for DySb and ErSb are listed in Table 3. Only theoretical values are available for Debye temperature for DySb and ErSb. Our values of Debye temperature of rare-earth antimonides show the same trend as reported by Mullen et al. [2]. Our calculated values of elastic constants are not in good agreement with Mullen's results because their values are at T=200 K temperature and our values are at T=0 K temperature.

An overall assessment shows that, in general, our values are close to available experimental data and are in general better matching than other theoretical data. The success

Table 3 Calculated values of elastic constants (in GPa) and bulk modulus (in GPa) of DySb and ErSb

Solid	DySb		ErSb	
	This work	Others	This work	Experimental
C_{11} (GPa)	120.67	141.74[a]	113.65	-
C_{12} (GPa)	19.8	25.86[a]	16.98	-
C_{44} (GPa)	22.36	26.22[a], 26.0[b]	19.57	26.0[b]
C_{11}–C_{12} (GPa)	100.87	148.0[b]	96.67	135.0[b]
B (GPa)	53.42	64.15	49.20	-
δ (GPa)	-2.56	-	-2.59	-
$_D$ (K)	263	241[b]	252	237[b]

[a] Ref [10]

[b] Ref [2] (at 200 K)

achieved in the present investigation can be ascribed to the inclusion of the covalency effect and charge transfer (or three body) as they seem to be of great importance at high pressure when the inter-ionic separation is reduced considerably and the coordination number increases. The successful predictions achieved from the present model in the present compounds can be considered remarkable in view of the fact that the model considered overlap repulsion effective up to second neighbor ions.

Finally, it may be concluded that the present MIPM model has successfully predicted the compression curves and phase diagrams giving the phase transition pressures, associated volume collapses and elastic properties correctly for these rare-earth antimonides. The inclusion of TBIs with covalency effects has improved the prediction of phase transition pressures over that obtained from the two-body potential and TBI without covalency. The use of a suitable functional form for three-body force parameter with covalency effect $f_m(r)$, instead of using it as a structure independent model parameter, might have improved the usefulness of the present model for estimating the actual high pressure behavior of the present compounds. Our results where no theoretical and experimental results are available may be tested with different theoretical and experimental methods and may be used to guide future work.

Acknowledgment P.B. is grateful to the Department of Science & Technology (DST), New Delhi for awarding WOS- 'A', and financial support to this work.

References

1. Duan CG, Sabirianov RF, Mei WN, Dowben PA, Jaswal SS, Tsymbal EY (2007) J Phys Condens Matter 19:315220–315252. doi:10.1088/0953-8984/19/31/315220
2. Mullen ME, Luthi B, Wang PS (1974) Phys Rev B 10:186–199. doi:10.1103/PhysRevB.10.186
3. Vaitheeswaran G, Kanchana V, Rajgopalan M (2002) Electronic and structural properties of LaSb and LaBi. Phys B 315:64–73. doi:10.1016/S0921-4526(01)01460-0
4. Vaitheeswaran G, Kanchana V, Rajgopalan M (2002) Theoretical study of LaP and LaAs at high pressures. J Alloys Compd 336:46–55. doi:10.1016/S0925-8388(01)01881-3
5. Lambrecht WPL (2000) Electronic structure and optical spectra of the semimetal ScAs and of the indirect-band-gap semiconductors ScN and GdN. Phys Rev B 62:13538–13545. doi:10.1103/PhysRevB.62.13538
6. Sera M (1983) Magnetic and transport properties of anomalous Ce-monopnictides. J Magn Magn Mater 31/34:385–386. doi:10.1016/0304-8853(83)90289-5
7. Ozeki S, Ohe Y, Kwon YS, Haga Y, Nakamura O, Suzuki T, Kasuya T (1991) Transport and magnetic properties of Sm monopnictides. Phys B 171:286–288. doi:10.1016/0921-4526(91)90533-K
8. Oyamada A, Ayache C, Suzuki T, Rossat-Mignod J, Kasuya T (1990) Transport properties of YbAs and YbP. J Magn Magn Mater 90/91:443–445. doi:0.1016/S0304-8853(10)80159-3
9. Li DX, Haga Y, Kwon YS, Shida H, Suzuki T, Nimori S, Kido G (1995) Resistivity and hall effect of GdSb and TmSb. J Magn Magn Mater 140/144:1165–1166. doi:10.1016/0304-8853(94)01016-1
10. Missell FP, Guertil RP, Foner S (1977) Magnetic properties of NdSb, GdSb, TbSb, DySb, HbSb and ErSb under hydrostatic pressure Solid. State Commmun 23:369–372. doi:10.1016/0038-1098(77)90234-4
11. Shapiro SM, Bak P (1975) Crystal field parameters and phase transitions in ErSb. J Phys Chem Solids 36:579–581. doi:10.1016/0022-3697(75)90145-6
12. Pagare G, Sen D, Srivastava V, Sanyal SP (2010) High pressure behavior of heavy rare earth monopnictides. J Phys Conf Ser 215:012114–012119. doi:10.1088/1742-6596/215/1/012114
13. Soni P, Pagare G, Sanyal SP (2010) A theoretical study of structural, elastic and thermal properties of heavy lanthanide monoantimonides. J Phys Chem Solids 71:1491–1498. doi:10.1016/j.jpcs.2010.07.014
14. Shirotani I, Yamanashi K, Hayashi J, Shimomura O, Kikegawa T (2003) Pressure induced phase transitions of lanthanides mono-arsenides LaAs and LuAs with a NaCl-type structure. Solid State Commmun 127:573–576. doi:10.1016/S0038-1098(03)00491-5
15. Shirotani I, Yamanashi K, Hayashi J, Tanaka Y, Ishimatsu N, Shimomura O, Kikegawa T (2001) Phase transitions of LnAs (Ln = Pr, Nd, Sm, Gd, Dy and Ho) with NaCl-type structure at high pressures. J Phys Condens Matter 13:1939–194. doi:10.1088/0953-8984/13/9/316
16. Shirotani I, Hayashi J, Yamanashi K (2001) Pressure-induced phase transitions in lanthanide monoantimonides with a NaCl-type structure. Phys Rev B 64:132101–132105. doi:10.1103/PhysRevB.64.132101
17. Sims CE, Barrera GD, Allan NL (1998) Thermodynamics and mechanism of the *B*1-*B*2 phase transition in group-I halides and group-II oxides. Phys Rev B 57:11164–11172. doi:10.1103/PhysRevB.57.11164
18. Rao BS, Sanyal SP (1991) High pressure structural phase transition in BaSe and BaTe. Phys Status Solidi b 165:369–375. doi:10.1002/pssb.2221650206
19. Froyen S, Cohen ML (1983) Structural properties of NaCl and KCl under pressure. J Phys C 19:2623–262. doi:10.1088/0022-3719/19/15/009
20. Singh RK (1982) Many body interactions in binary ionic solids. Phys Rep 85:259–401. doi:10.1016/0370-1573(82)90020-5
21. Motida K (1986) Effect of covalency on Phonon dispersion relations in NaCl type Alkali Halide crystals. J Phys Soc Jpn 55:1636–1649. doi:10.1143/JPSJ.55.1636
22. Bhardwaj P, Singh S, Gaur NK (2008) Structural and elastic properties of barium chalcogenides (BaX, X=O, Se, Te) under high pressure. J Cetr Euro J Phys 6:223–229. doi:10.2478/s11534-008-0011-7
23. Bhardwaj P, Singh S, Gaur NK (2009) Structural, elastic and thermophysical properties of divalent metal oxides with NaCl structure. Mater Res Bull 44:1366–1374. doi:10.1016/j.materresbull.2008.12.012
24. Singh RK, Singh S (1989) Structural phase transition and high-pressure elastic behavior of III-V semiconductors. Phys Rev B Condens Matter 39:671–676. doi:10.1103/PhysRevB.39.671
25. Sharma UC, Verma MP (1980) On the pressure derivatives of the second-order elastic constants of ionic solids. Phys Status Solidi b 102:487–494. doi:10.1002/pssb.2221020206
26. Sharma UC (1985) On the pressure dependence of mechanical behavior ionic solids. PhD Thesis. Agra University, Agra
27. Lide DR (1995–1996) Handbook of chemistry and physics. CRC 12:21–24